1	Supplementary Material for
2	Seismica
3	
4	Bayesian Reassessment of Seismic Moment Tensor and Their
5	Uncertainties in the Adriatic Sea Region
6	Jinyin Hu ^{1,*} , Hrvoje Tkalčić ¹ , Thanh-Son Phạm ¹ , Marijan Herak ² , Iva Dasović ² , Marija Mustać Brčić ²
7 8 9 10	¹ Research School of Earth Sciences, The Australian National University, Canberra, ACT, Australia ² Department of Geophysics, Faculty of Science, University of Zagreb, Zagreb, Croatia *Corresponding author: Jinyin.hu@anu.edu.au
11	Introduction
12	This supplemental material contains a description of the station selection scheme and Figures
13	S1- S13 to support the discussion in the main text.
14	
15	We modified the station selection method of Ekström (2006) for our inversion by adding the
16	weight for epicenter distance. First, all available stations are assigned a score (Eq. 3) based on
17	the SNR and the epicenter distance weighting \overline{D} as
18	$\overline{D} = \begin{cases} 0.25, & \text{if } d \le 50 \text{ km} \\ 0.75, & \text{if } d \in (50,130] \text{ km} \\ 1.0, & \text{if } d \in (130,220] \text{ km} \end{cases} (S1),$ $0.5, & \text{if } d > 220 \text{ km} \end{cases}$
19	where d is the epicenter distance. To balance the SNR and \overline{D} , we normalized the SNR values
20	by their maximum across all stations. Stations were then ranked according to their scores in
21	Eq. 3 with higher scores assigned higher ranks and lower scores assigned lower ranks. The
22	first station was selected as the one with the highest rank (i.e., the highest station score). For
23	the second station, we evaluated all remaining stations by considering their contribution to
24	azimuthal coverage, quantified using the effective number of stations (ENS) as defined in Eq.
25	10 of Ekström (2006). Specifically, we computed the ENS for each remaining station in
26	combination with the already selected first station and ranked them by their ENS values
27	(Rank2). We also updated their original station-score-based ranking (Rank1) to reflect the
28	reduced number of remaining stations after each selection. The two ranks were then summed
29	for each station, and the station with the highest combined rank was selected as the second
30	station. This process was repeated iteratively until the required number of stations was
31	selected.

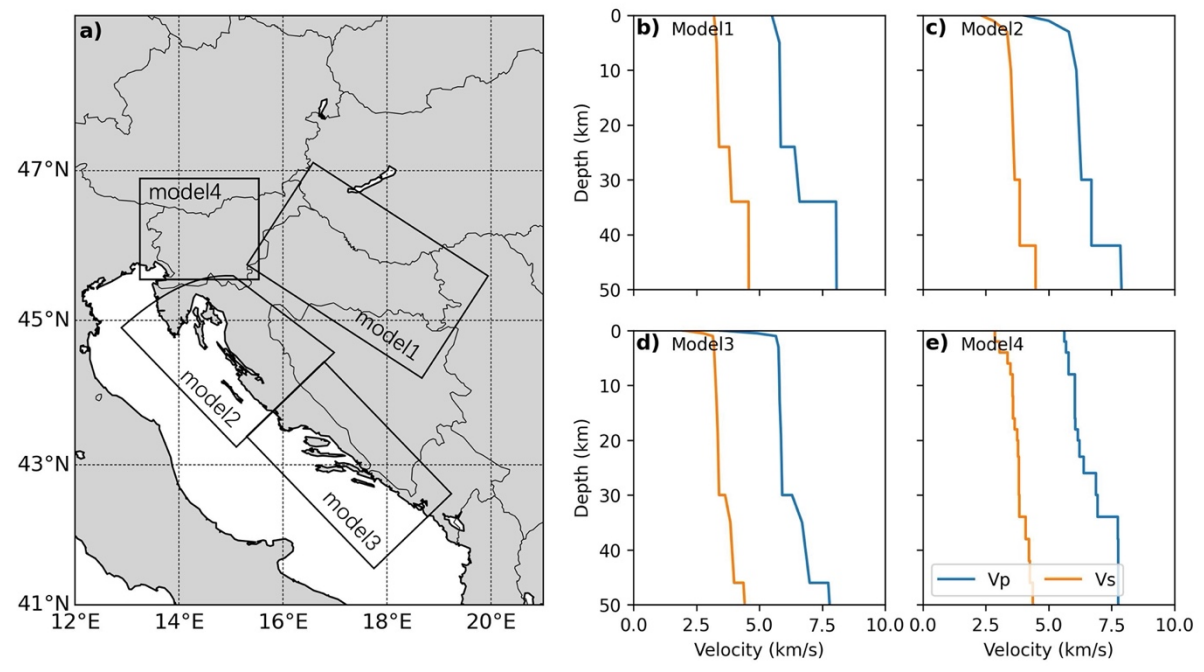


Figure S1 The 2-D velocity models used for the region surrounding Croatia. Models 1, 2, and 3 are 1D velocity models obtained from the receiver function (Stipčević et al., 2011, 2020). Model 4 is the 1D velocity model for the northwestern Dinarides from Rajh et al. (2022).

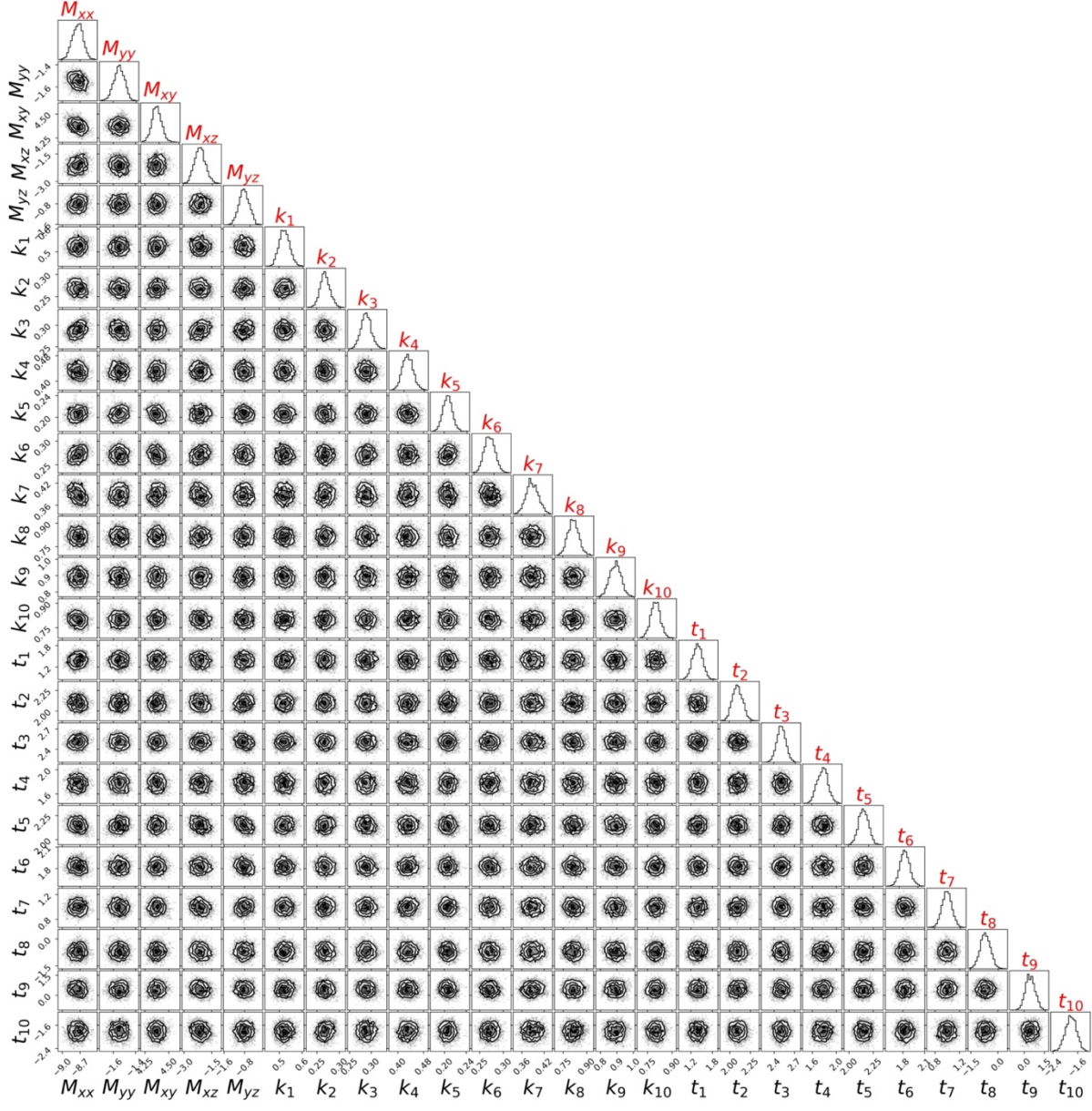


Figure S2 Posterior distribution of unknown parameters in the Bayesian MT inversion for the largest aftershock of the 2020 Zagreb earthquake (Event 2). The unit of MT parameters is 10¹⁵ Nm. See the caption of Fig. 3 for details.

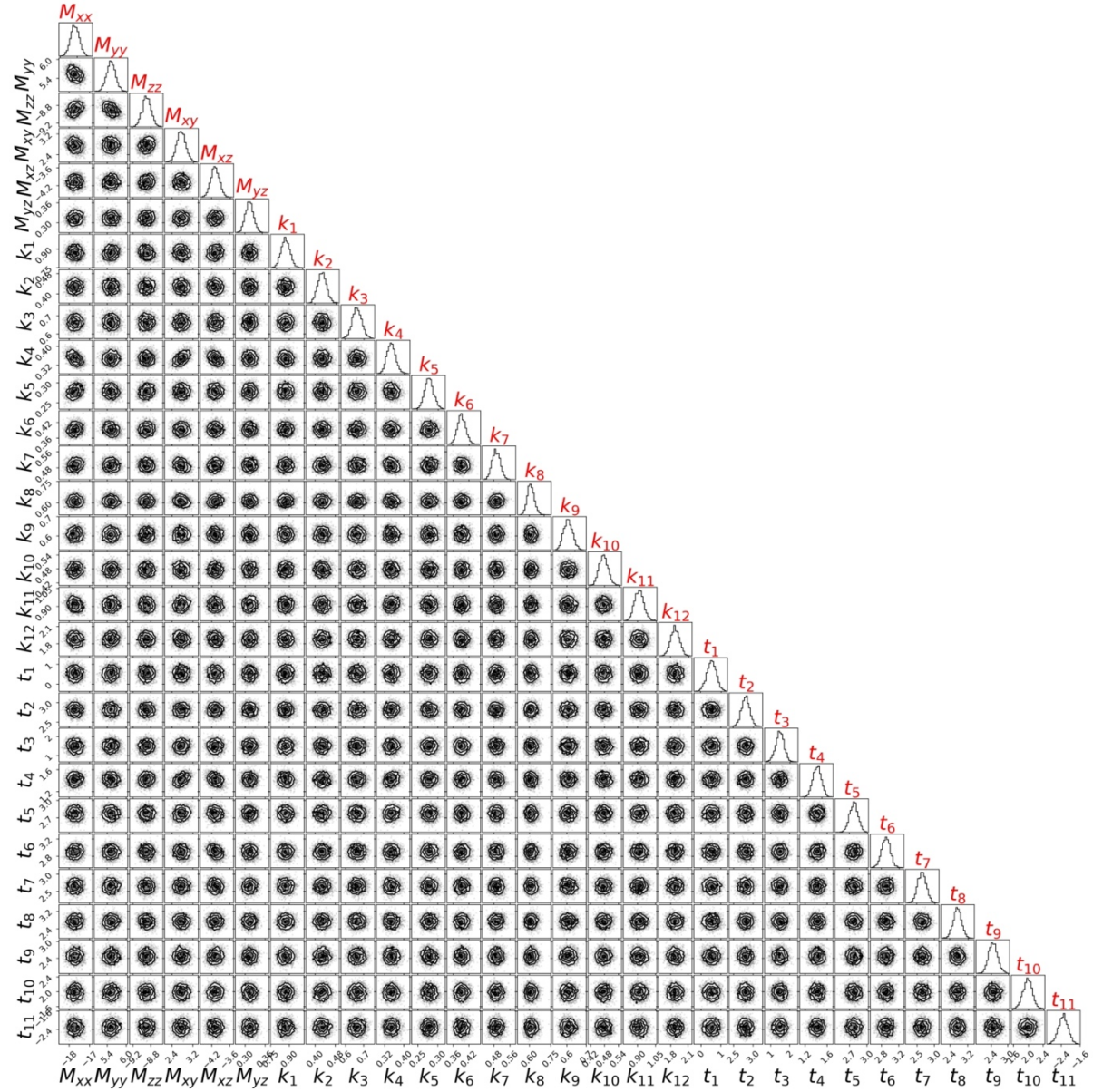


Figure S3 Posterior distribution of unknown parameters in the Bayesian MT inversion for the largest foreshock of the 2020 Petrinja earthquake (Event 3). The unit of MT parameters is 10¹⁵ Nm. See the caption of Fig. 3 for details.

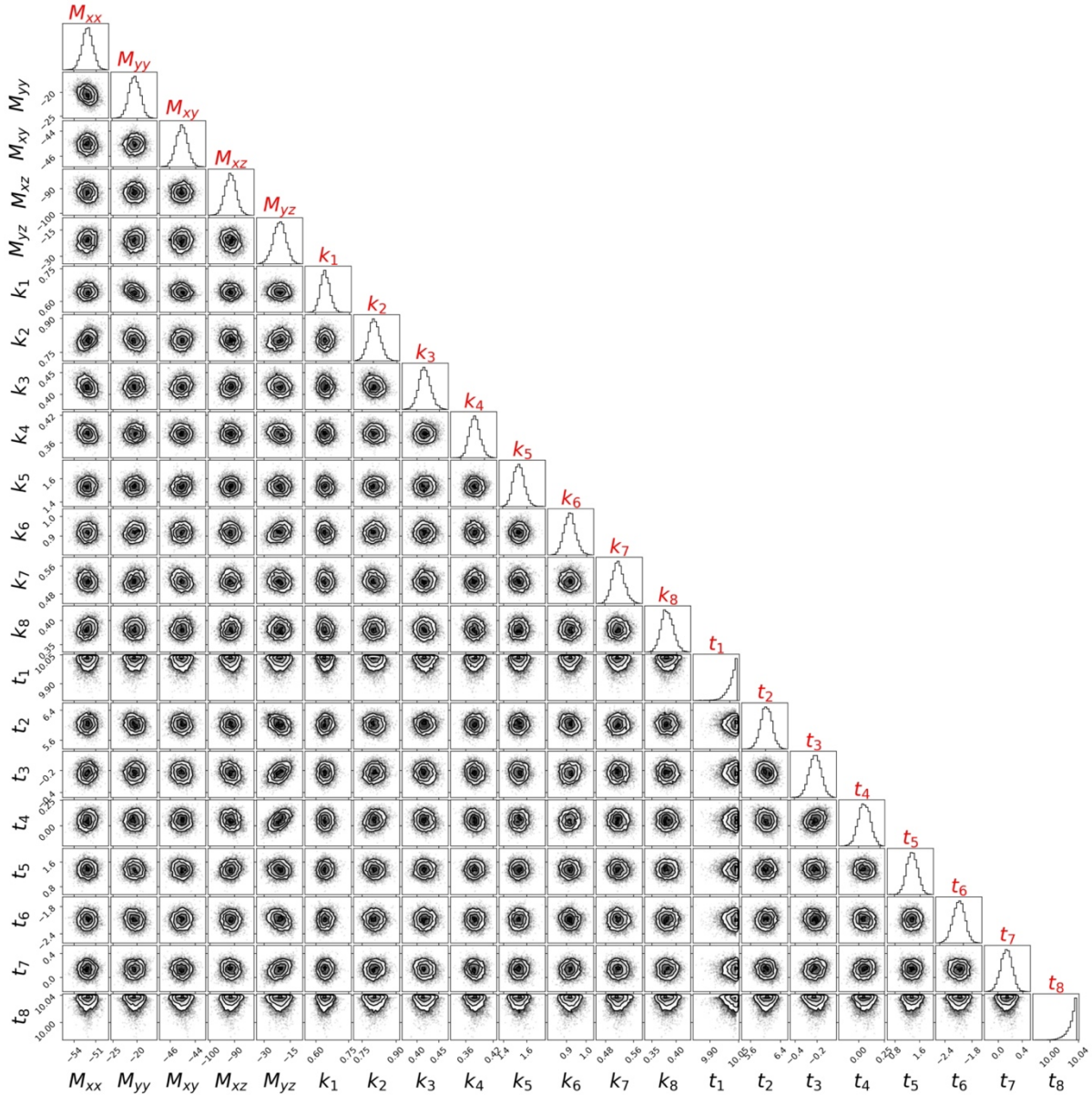


Figure S4 Posterior distribution of unknown parameters in the Bayesian MT inversion for the 2021 central Adriatic earthquake (Event 4). The unit of MT parameters is 10¹⁵ Nm. See the caption of Fig. 3 for details.

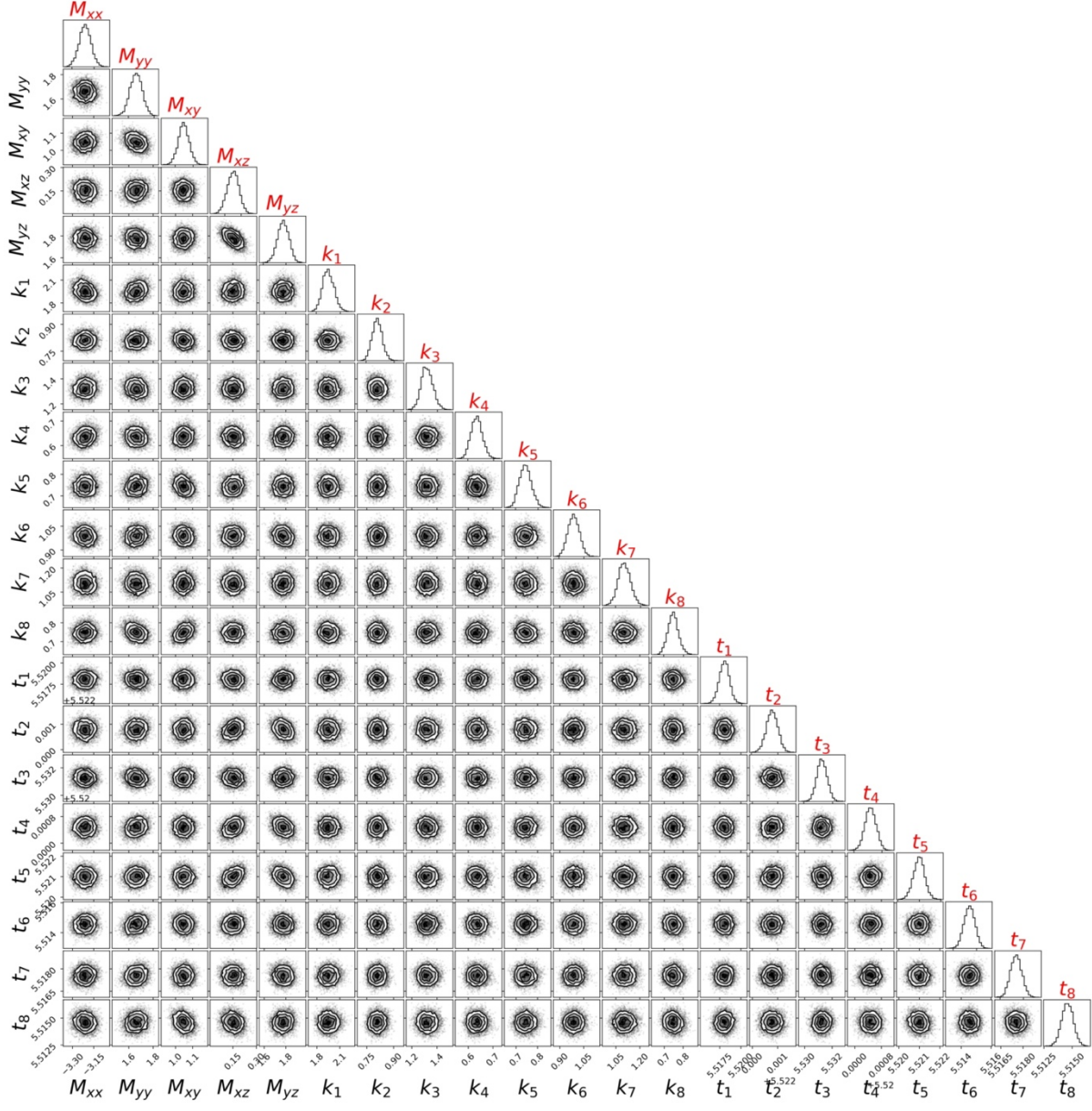


Figure S5 Posterior distribution of unknown parameters in the Bayesian MT inversion for the 2024 southern Adriatic earthquake (Event 5). The unit of MT parameters is 10¹⁵ Nm. See the caption of Fig. 3 for details.

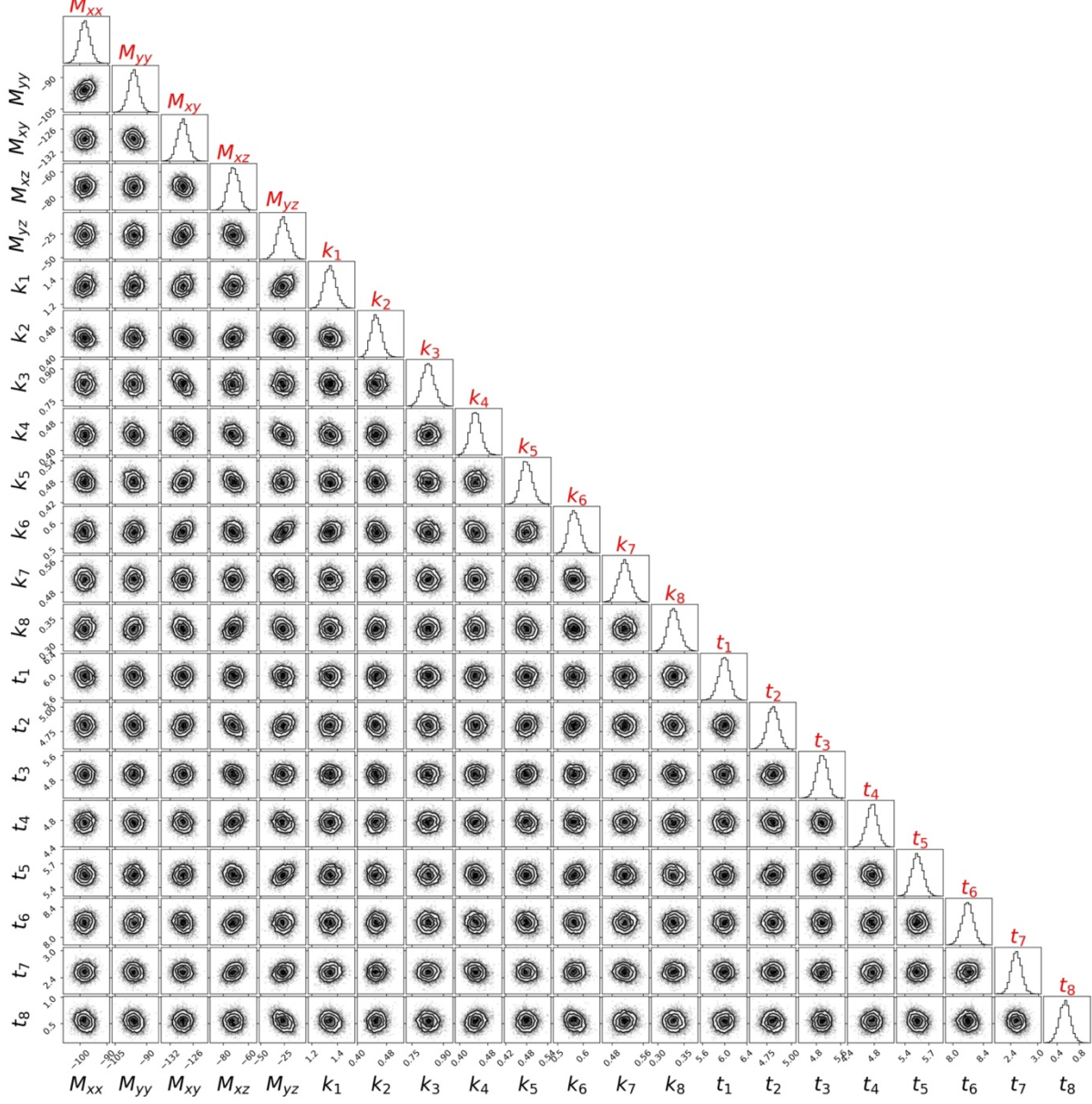


Figure S6 Posterior distribution of unknown parameters in the Bayesian MT inversion for the 2022 earthquake in Costa Marchigiana Pesarese (Event 6). The unit of MT parameters is 10¹⁵ Nm. See the caption of Fig. 3 for details.

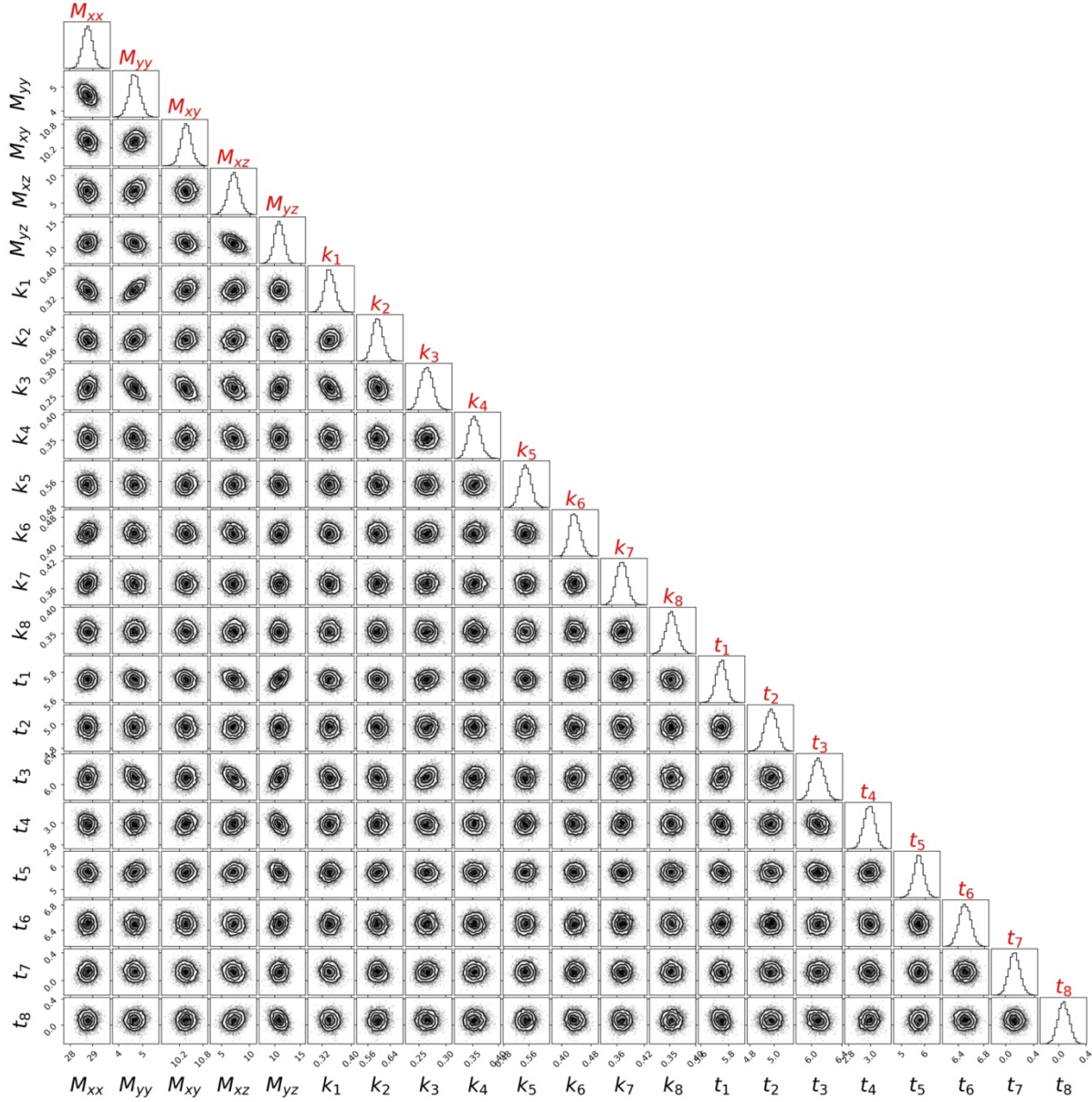


Figure S7 Posterior distribution of unknown parameters in the Bayesian MT inversion for the 2023 earthquake in Marradi, Tuscany (Event 7). The unit of MT parameters is 10¹⁵ Nm. See the caption of Fig. 3 for details.

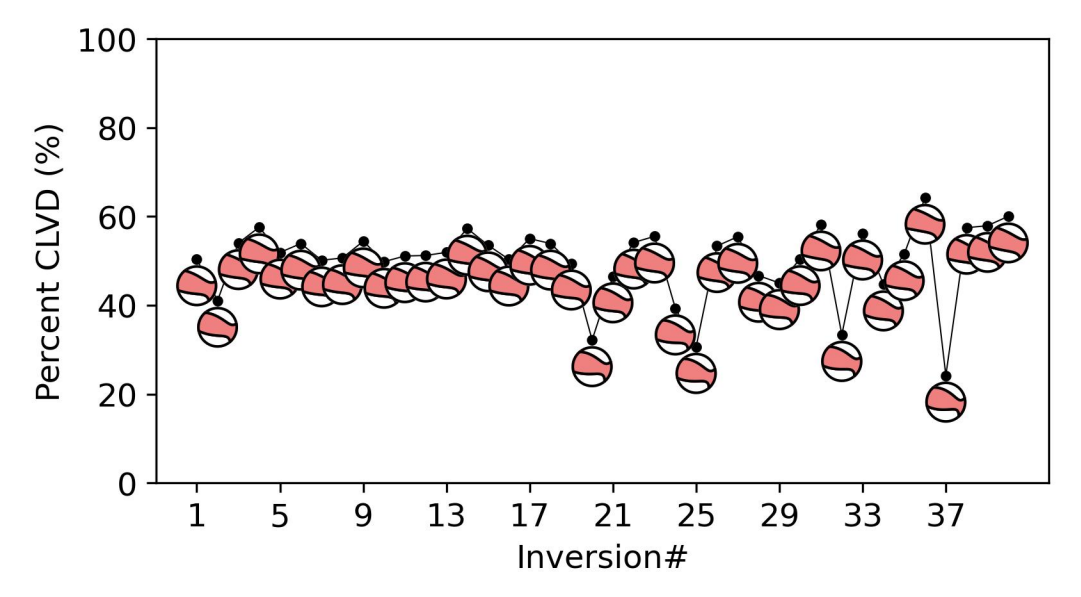


Figure S8 The sensitivity test for Event 3. We randomly discard 1, 2, 3, 4, or 5 stations from the 12 stations and repeat 8 times, resulting in 40 inversions here. The beachball represents the mean MT solution from each inversion. The mean percentage of CLVD is 50.1%.

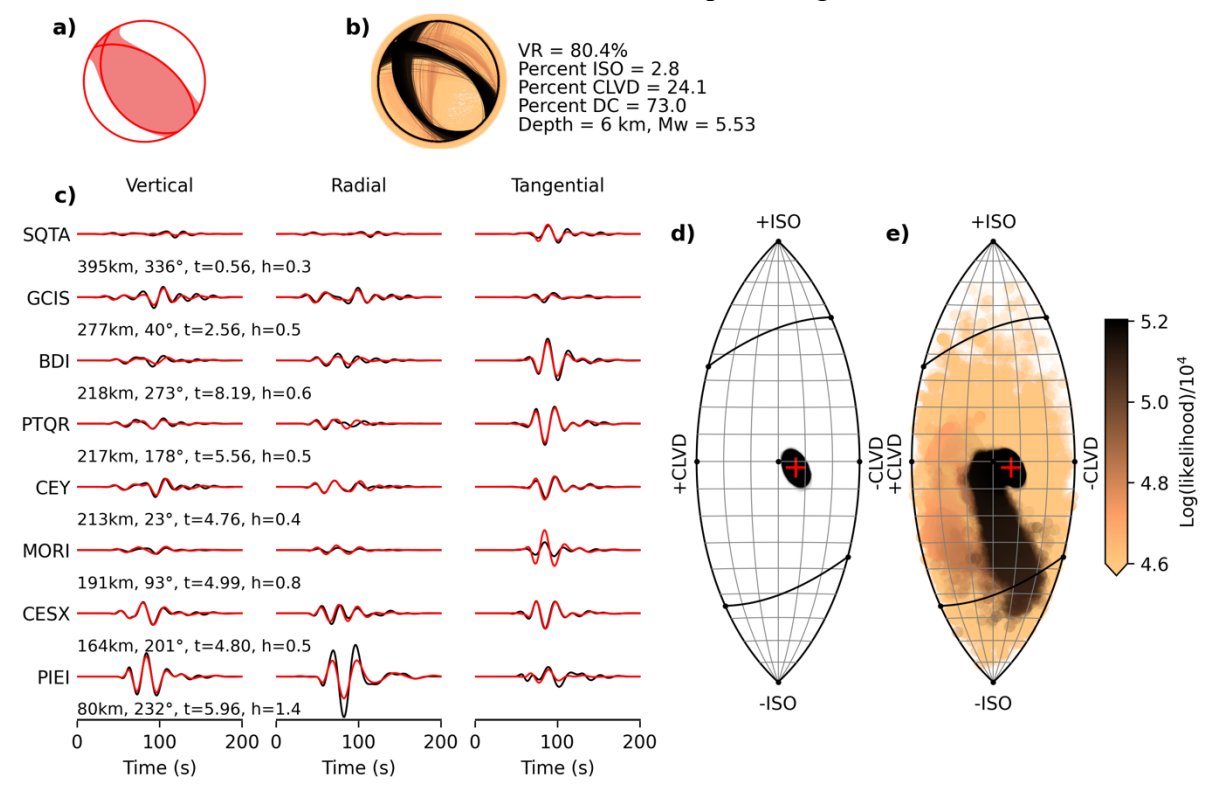
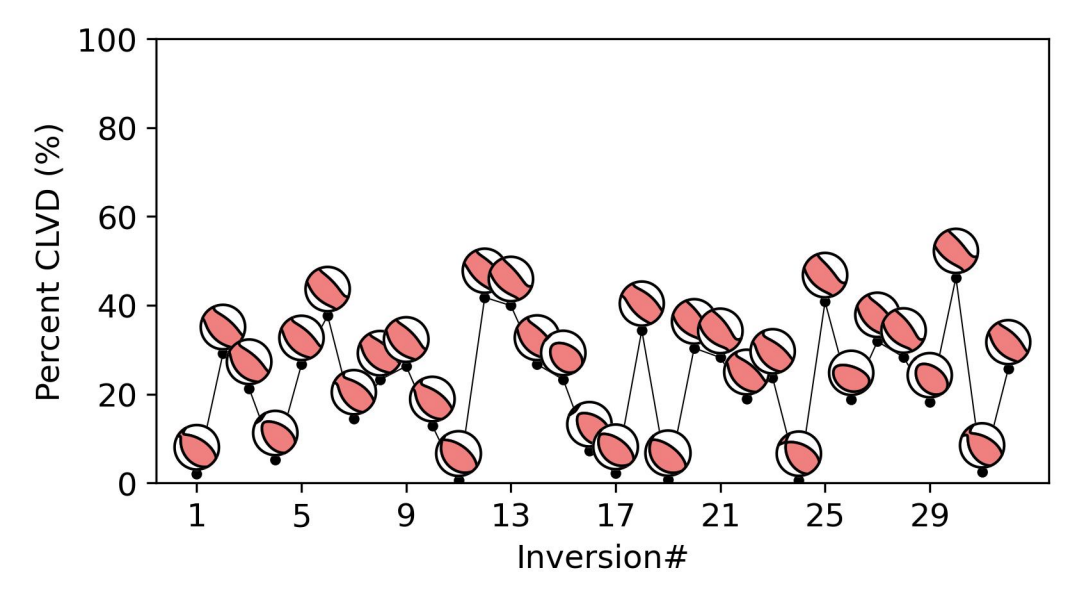


Figure S9 Full MT inversion for the 2022 earthquake in Costa Marchigiana Pesarese (Event 6). See the caption of Fig. S8 for details.



 $\begin{array}{c} 103 \\ 104 \end{array}$

Figure S10 The sensitivity test for Event 6. We randomly discard 1, 2, or 3 stations from the 8 stations and repeat 8 times, resulting in 24 inversions here. The beachball represents the mean MT solution from each inversion. The mean percentage of CLVD is 21.55%.

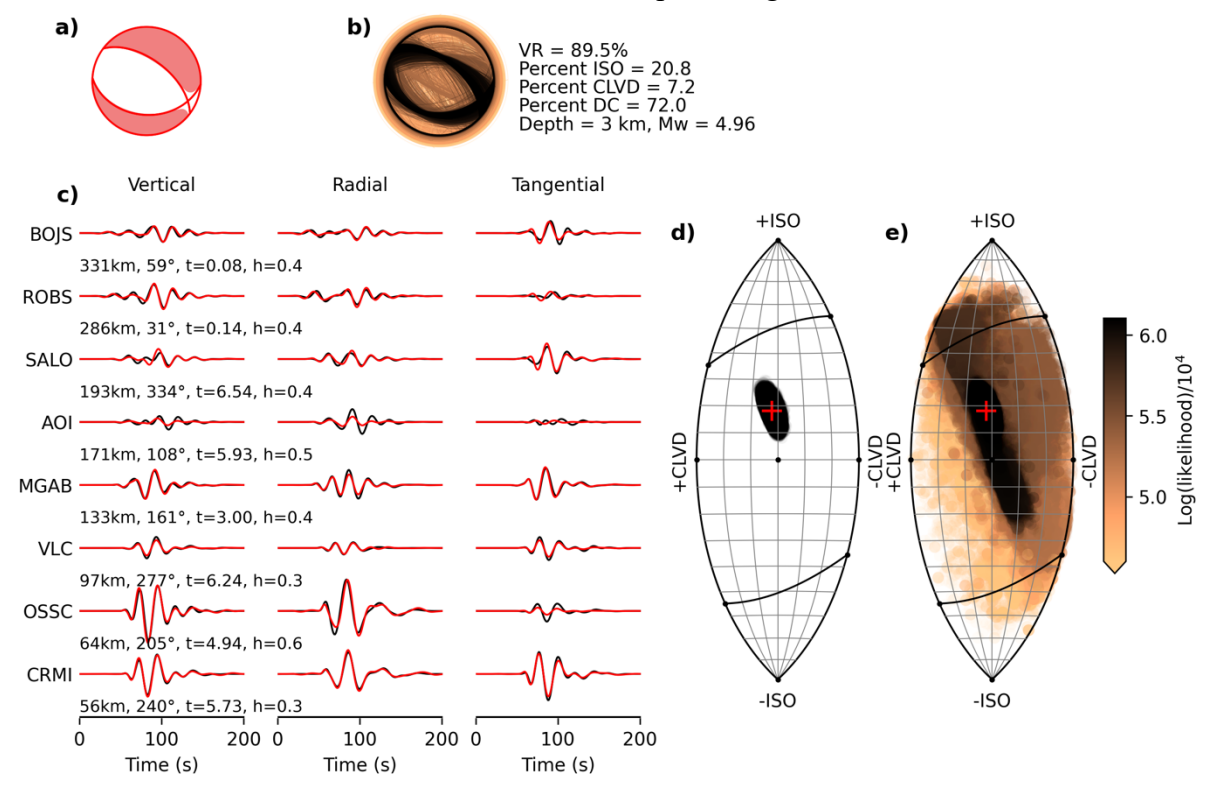


Figure S11 Full MT inversion for the 2023 $M_w4.9$ earthquake in Marradi, Tuscany (Event 7). See the caption of Fig. S8 for details.

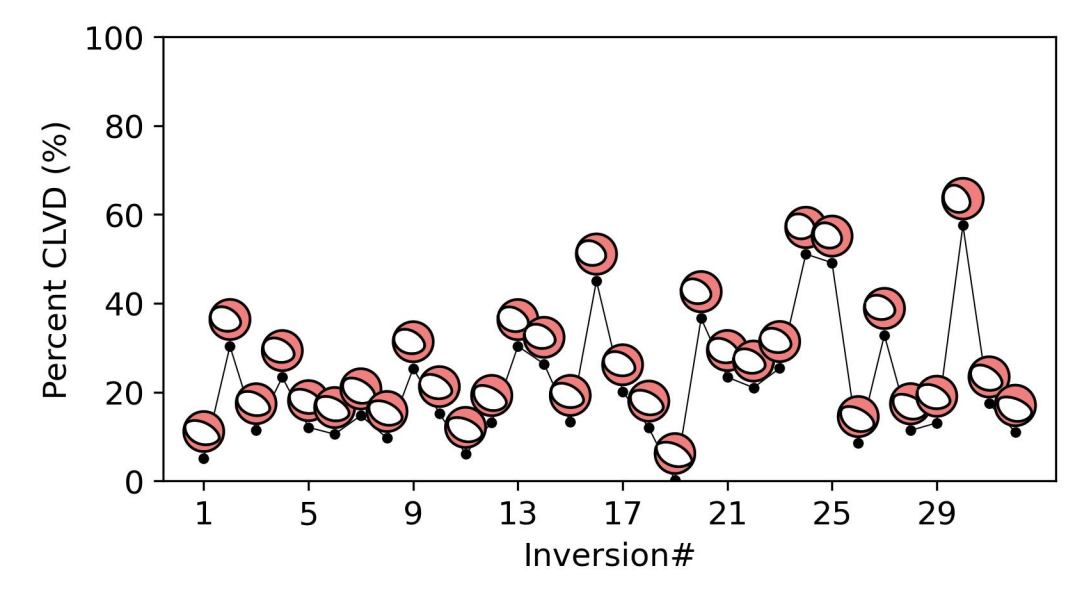


Figure S12 The sensitivity test for Event 7. We randomly discard 1, 2, or 3 stations from the 8 stations and repeat 8 times, resulting in 24 inversions here. The beachball represents the mean MT solution from each inversion. The mean percentage of CLVD is 21.33%.

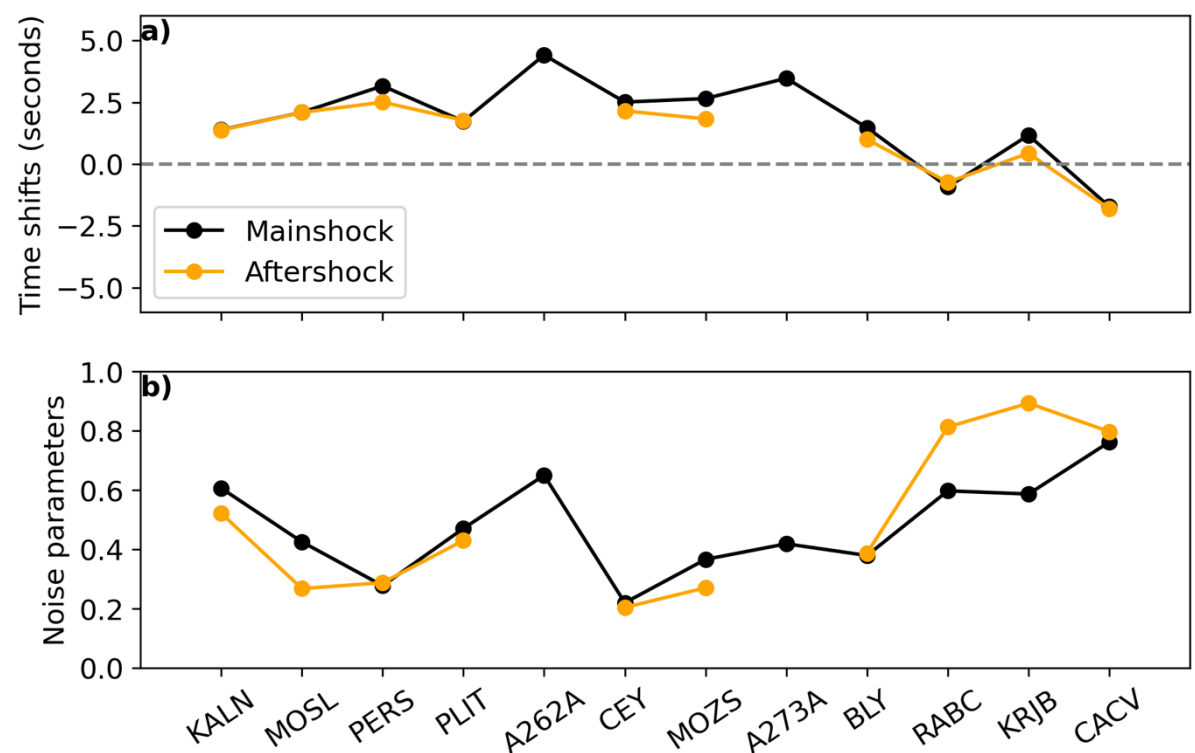


Figure S13 Plot of station-specific time shifts (a) and data noise (b) from the MT inversions in Figs. 2 and 4 for the mainshock (black) and aftershock (yellow) of the 2022 Zagreb earthquake, respectively.

References

Ekström, G. (2006). Global Detection and Location of Seismic Sources by Using Surface Waves. *Bulletin of the Seismological Society of America*, *96*(4A), 1201–1212. https://doi.org/10.1785/0120050175

122	Rajh, G., Stipčević, J., Zivčić, M., Herak, M., Gosar, A., & the AlpArray Working Group.
123	(2022). One-dimensional velocity structure modeling of the Earth's crust in the
124	northwestern Dinarides. Solid Earth, 13(1), 177-203. https://doi.org/10.5194/se-13-
125	177-2022
126	Stipčević, J., Tkalčić, H., Herak, M., Markušić, S., & Herak, D. (2011). Crustal and
127	uppermost mantle structure beneath the External Dinarides, Croatia, determined from
128	teleseismic receiver functions: Crustal structure in the External Dinarides.
129	Geophysical Journal International, 185(3), 1103–1119.
130	https://doi.org/10.1111/j.1365-246X.2011.05004.x
131	Stipčević, J., Herak, M., Molinari, I., Dasović, I., Tkalčić, H., & Gosar, A. (2020). Crustal
132	Thickness Beneath the Dinarides and Surrounding Areas From Receiver Functions.
133	Tectonics, 39(3), e2019TC005872. https://doi.org/10.1029/2019TC005872
134	